How to cite: *Angew. Chem. Int. Ed.* **2023**, *62*, e202308857
doi.org/10.1002/anie.202308857

Liquid Crystals

Liquid Crystal Emulsions: A Versatile Platform for Photonics, Sensing, and Active Matter

*Alberto Concellón**

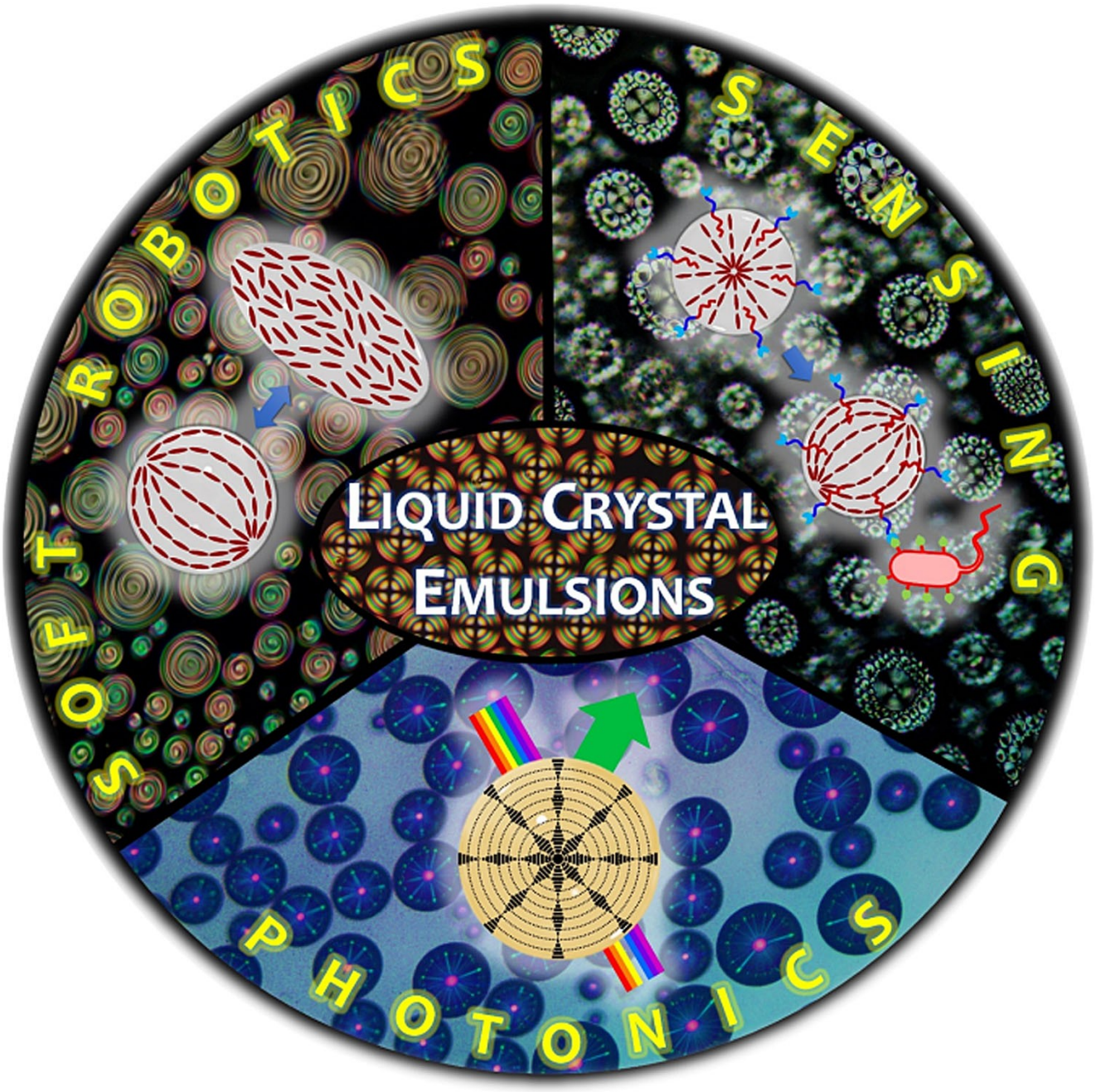

Angewandte International Edition Chemie

Abstract: The self-assembly of liquid crystals (LCs) is a fascinating method for controlling the organization of discrete molecules into nanostructured functional materials. Although LCs are traditionally processed in thin films, their confinement within micrometre-sized droplets has recently revealed new properties and functions, paving the way for next-generation soft responsive materials. These recent findings have unlocked a wealth of unprecedented applications in photonics (e.g. reflectors, lasing materials), sensing (e.g. biomolecule and pathogen detection), soft robotics (e.g. micropumps, artificial muscles), and beyond. This Minireview focuses on recent developments in LC emulsion designs and highlights a variety of novel potential applications. Perspectives on the opportunities and new directions for implementing LC emulsions in future innovative technologies are also provided.

1. Introduction

Liquid crystals (LCs) are fascinating, stimuli-responsive soft materials that combine the mechanical characteristics of liquids with the anisotropic properties of crystals. LC molecules (so-called mesogens) exhibit orientational and several degrees of translational/positional order, while maintaining their liquid fluidity (Figure 1).[1] LCs are considered stimuli-responsive smart materials, where an external stimulus (e.g., temperature, electric field, light, mechanical stress, etc.) can induce molecular-level changes in the order and/or orientation of the mesogens. These changes propagate to the macroscopic level, thereby altering the properties of the LC material.[2] The intrinsic anisotropy of LCs, combined with the ease of reorientation and alignment manipulation, forms the basis for several commercial applications, including flat panel displays (i.e., LCD TVs), thermometers, personal protective equipment (i.e., Kevlar), or heat sensitive cameras. The self-assembly of LCs is an interesting approach for directing the arrangement of molecules into an array of nanostructures, including columnar, smectic, or bicontinuous cubic LC phases. These LC phases are used to construct a variety of functional materials that provide effective solutions for recent challenging problems, such as electron/ion transport for energy applications, separation for environmental remediation, opto-electronics, sensing, or soft robotics.[3]

Although thermotropic LCs are traditionally processed in solid film slabs, interesting physical phenomena arise when they are confined within micrometre-sized emulsion droplets.[4] An intriguing phenomenon, for instance, is the extreme sensitivity of the LC orientational order in proximity to interfaces. This sensitivity leads to molecular-level interactions occurring at the interface being transmitted from the boundary into the bulk, generating novel structures characterized by controllable topological defects and dislocations. The first example of confined LCs was "polymer-dispersed LCs" (PDLCs) and consisted of nematic LC micrometer-sized droplets embedded in a continuous polymeric matrix. PDLCs were successfully employed in the fabrication of electro-optical devices (e.g., displays, light shutters, smart windows…) due to their LC orientation-dependent optical properties that could be readily switched between ON (transparent) and OFF (opaque) states by applying external fields. Apart from PDLCs, there has been a growing interest in spherical confinements of LCs at liquid-liquid interfaces, especially those LCs dispersed in water and decorated with surfactants. These systems have opened up new opportunities for the design of complex soft responsive materials and have enabled a wealth of unprecedented applications in photonics, sensing, or soft robotics.[5]

This Minireview aims to provide an overview on the recent findings in LC emulsions, focusing on a variety of novel designs and their potential applications. Section 2 discusses various methods for preparing of LC droplets, highlighting how to control the LC configuration within these droplets. While there have been several reported applications of LC emulsions, section 3 highlights recent developments through selected examples, such as LC emulsion-based chemical and biological sensors, mechanical actuators, or photonic systems. These potential applications

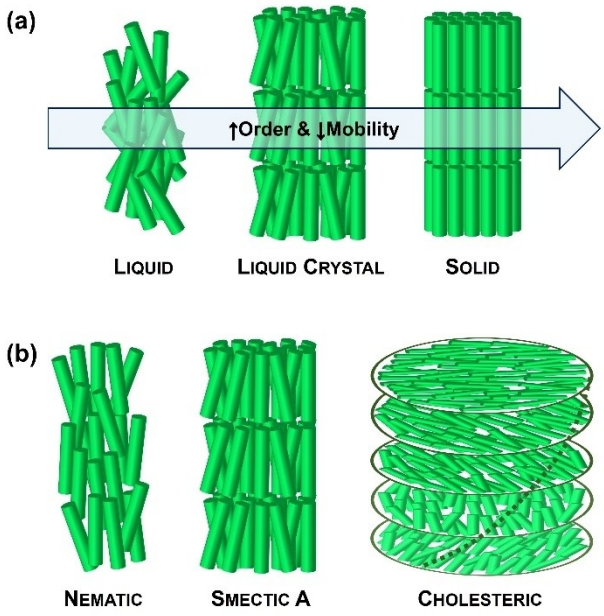

Figure 1. **(a)** Organization of molecules in the liquid, LC, and solid states. **(b)** Examples of commonly used LC phases in LC emulsions.

[*] Dr. A. Concellón
Instituto de Nanociencia y Materiales de Aragón (INMA),
CSIC-Universidad de Zaragoza
C/Pedro Cerbuna 12, 50009 Zaragoza (Spain)
E-mail: aconcellon@unizar.es

were selected to illustrate the versatility and smart nature of LC emulsions, which have opened new frontiers in designing functional soft materials. To conclude this Minireview, section 4 focuses on the challenges, opportunities, and new directions for advancing in functional materials and devices based on LC emulsions.

2. Liquid Crystal Emulsion Fabrication and Their Internal Configuration

2.1. Production Methods for Liquid Crystal Droplets

Emulsions are thermodynamically unstable mixtures of two or more immiscible liquids. Emulsions do not form spontaneously; they need an energy input and the application of emulsifying agents to prompt the dispersion of droplets within the continuous phase.[6] LC emulsions are typically prepared using similar fabrication methods to those employed for isotropic emulsions.[7]

The simplest technique to produce LC emulsions is bulk emulsification and consists of applying high-shear forces using mechanical devices such as vortex mixers, homogenizers, ultrasonicators, or gentle hand shaking (Figure 2a).[8] These mechanical methods induce the fragmentation of the LC oil into micrometer-sized droplets, leading to emulsions with minimal coalescence as the newly produced LC droplets are sufficiently dilute in the continuous phase. Bulk emulsification is a relatively fast process (taking only a few minutes), but it generates polydisperse droplets with sizes ranging from 0.1 to 500 μm. Despite this polydispersity, the desired range of droplet sizes can be achieved through careful selection of the mechanical device used for bulk emulsification. Vortexing is unsuitable for viscous continuous phases (e.g., glycerol) and yields relatively large droplet sizes (around 100 μm), which can be somewhat controlled by adjusting the vortexing speed. Ultrasound generators readily generate droplets that are typically from 0.1 to 10 μm, whereas homogenizers form droplets with diameters between 1 to 50 μm.

Alberto Concellón obtained his Ph.D. in Chemistry from the University of Zaragoza in 2018, where he worked in Prof. Serrano's group on the synthesis of functional liquid crystalline materials. During that time, he also spent time at the Eindhoven University of Technology (Prof. Schenning) and at the University of Calabria (Prof. Golemme). In 2018, he joined Prof. Swager's group at the Massachusetts Institute of Technology as a postdoc, working on complex smart colloids, chemical sensors, and chiroptical materials. After 4 years at MIT, he returned to the University of Zaragoza as a Ramón y Cajal Fellow. His research is focused on innovative designs of functional self-assembled materials.

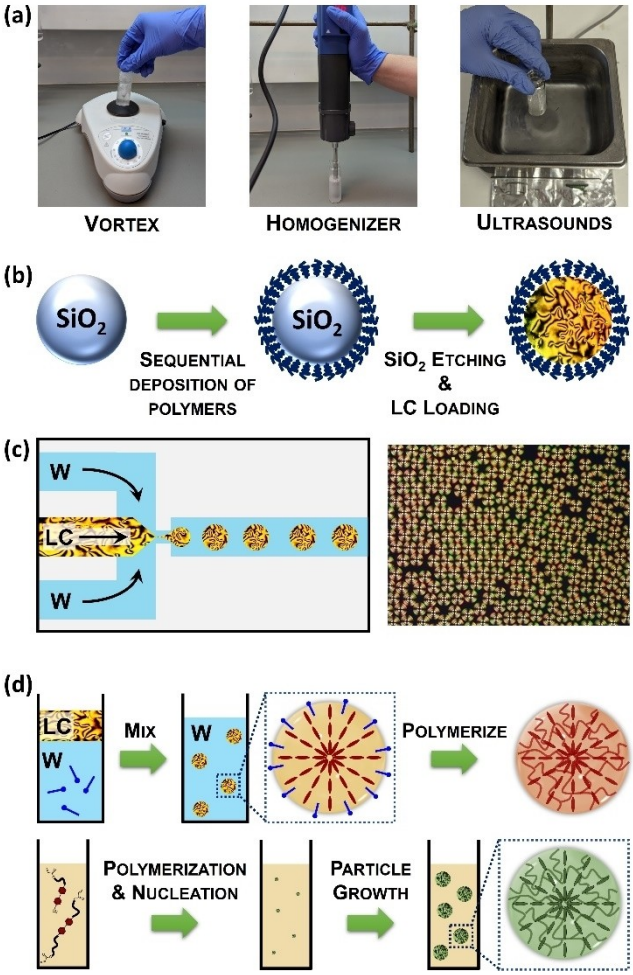

Figure 2. Methods for the production of LC droplets: **(a)** emulsification using a vortex, homogeneizer or an ultrasonicator, **(b)** encapsulation of a LC within polyelectrolyte capsules, **(c)** microfluidics for producing monodisperse LC droplets, **(d)** suspension (top) and precipitation polymerization (bottom).

A more precise method for bulk emulsification was described by Abbott, Caruso and co-workers.[9] Their approach is based on the templated synthesis of polyelectrolyte capsules using sacrificial silica microparticles, followed by filling of the hollow capsules with the LC (Figure 2b). This method enables the production of large quantities of LC droplets with narrow size distributions due to the possibility of preparing silica particles with monodisperse sizes. Additionally, polyelectrolyte capsules can be easily decorated with a diverse array of functional polymers, providing access to LC emulsions with a controlled interfacial chemistry.

Microfluidics has found widespread application in producing highly uniform emulsion droplets with precise monodispersity and finely tunable sizes (10–100 μm) at a remarkable rate of approximately 25,000 droplets per second (Figure 2c).[10] In addition to LC single emulsions (i.e., a LC confined in spherical droplets that are dispersed in a liquid), microfluidic techniques also facilitate the generation of multi-compartment emulsion droplets featur-

ing well-defined volumes and compositions, including water-in-LC-in-water (W/LC/W; so-called shells), Janus emulsions, LC-in-fluorocarbon-in-water (LC/F/W), or fluorocarbon-in-LC-in-water (F/LC/W), among others.

Classical polymerization techniques provide an alternative for creating LC droplets with smaller sizes (<10 μm) (Figure 2d).[11] Precipitation polymerization is probably the most interesting method since it allows the preparation of nearly monodisperse LC polymer droplets with diameters of ≈ 1 μm.[12] Precipitation polymerization starts with a homogeneous solution of reactive LC monomers. As polymerization occurs, newly formed polymer chains precipitate, forming initial particles that subsequently grow to yield the final LC particles. In contrast, suspension and mini-emulsion polymerization involve the dispersion of a mixture of LC monomers in the continuous phase via bulk emulsification, followed by polymerization. Both methods are compatible with a wide range of LC phases and enable the preparation of LC polymer particles with broad size distributions and with average diameters of >1 μm for suspension polymerization, or <1 μm for mini-emulsion polymerization.

Despite yielding LC droplets in all instances, the aforementioned methods diverge in terms of droplet size distributions and usability. Multiple factors can impact the characteristics of LC droplets, one of which is the inclusion of surfactants. The use of surfactants significantly diminishes the size of LC droplets; however, it also influences the internal LC configuration within droplets (vide infra). Thus, meticulous control of surfactant concentration is also essential.

2.2. Internal Configurations of Liquid Crystal Droplets

The most challenging issue in preparing LC emulsions is the control of mesogens organization at interfaces, resulting in a variety of LC internal configurations that display distinct optical signatures when studied by polarized-light optical microscopy.[13] Such optical textures permit the identification of the organization of the confined LC, which is typically governed by a subtle energetic balance that involves contributions arising from the interfacial and elastic energies of the LC, or the presence of topological defects.[5b]

The nematic LC phase, in which mesogens have only orientational order (Figure 1b), has been the most widely used phase within droplets. In this phase, mesogens can align either parallel (planar) or perpendicular (homeotropic) to the interface, leading to bipolar or radial configurations, respectively (Figure 3a). In a planar configuration two diametrically opposed surface point defects are present at the poles, whereas in a radial configuration a single point defect appears in the center of the droplet.[14] By tilting the surface anchoring of mesogens from planar to homeotropic, additional intermediate LC configurations can be obtained, such as axial, pre-radial, or escaped radial. Although there are several factors that govern the alignment of mesogens within nematic droplets (e.g., droplet size, surfactant type, concentration…), the LC configuration of droplets with sizes >10 μm can be readily controlled by a proper choice of surfactants.[15] For instance, surfactants containing long alky chains extend their hydrophobic alkyl chain perpendicular to the LC/W interface, making mesogens align homeotropically and leading to a radial configuration. Examples of these surfactants include sodium dodecyl sulfate (SDS), hexadecyltrimethylammonium bromide (CTAB), or polysorbate-type surfactants (Tween). Nonetheless, polymeric surfactants, such as polyvinylalcohol (PVA) or polyvinylpyrrolidone (PVP), absorb at the LC/W interface in a random coil conformation, making mesogens align parallel to the aqueous interface and producing a bipolar configuration.[2b]

LC droplets comprising smectic mesophases have also been prepared.[16] Smectic phases are lamellar arrangements, in which mesogens present both orientational and a position order in layers (Figure 1b). This lamellar organization imposes additional constrains on mesogens organization, affects the defect configuration, and leads to emulsions with more complex internal organizations than those observed with nematic LCs.

The introduction of chirality into a nematic LC phase produces twisting of the mesophase director, leading to chiral nematic LCs (so-called cholesteric LCs) (Figure 1b). Cholesteric LCs have been widely employed for the preparation of LC droplets since they are considered 1D photonic materials that reflect light due to their periodic helical configuration. Controlling the anchoring conditions at interfaces is critical to create cholesteric LC droplets with well-defined internal helical arrangements.[17] The most interesting organization originates when mesogens align parallel (planar) to the aqueous interface, resulting in a radial distribution of the helical axes (Figure 3b). This internal configuration leads to cholesteric LC droplets with enhanced photonic properties (i.e., omnidirectional light reflection). Cholesteric LC shells have also been prepared, wherein a planar anchoring of the mesogens at both aqueous interfaces (i.e., the inner and surrounding aqueous phases) is required to achieve a radial helical organization. Aqueous solutions of PVA, PVP, or glycerol are the most widely used continuous phases to achieve radial helical arrangements.

Complex emulsions comprising immiscible nematic LCs and fluorocarbon oils were also described by Swager and co-workers (Figure 3c).[18] The presence of an additional interface provides additional topological constrains that can be controlled by using appropriately designed surfactants to provide specific anchoring of the mesogens at each interface. Complex LC emulsions exhibiting different internal configurations were prepared, and the morphology of these complex emulsions could be switched between LC/F/W double emulsions, Janus emulsions, and F/LC/W double emulsions. Complex LC emulsions with intricate internal arrangements were also prepared using both smectic and cholesteric phases.[18b,19] Moreover, non-spherical structures with complex internal LC organizations were generated through polymerization techniques. For instance, Schenning and co-workers described flower-like morphologies, in which the particle size and the number of "petals" per particle can be adjusted by modifying the emulsion polymerization conditions.[20]

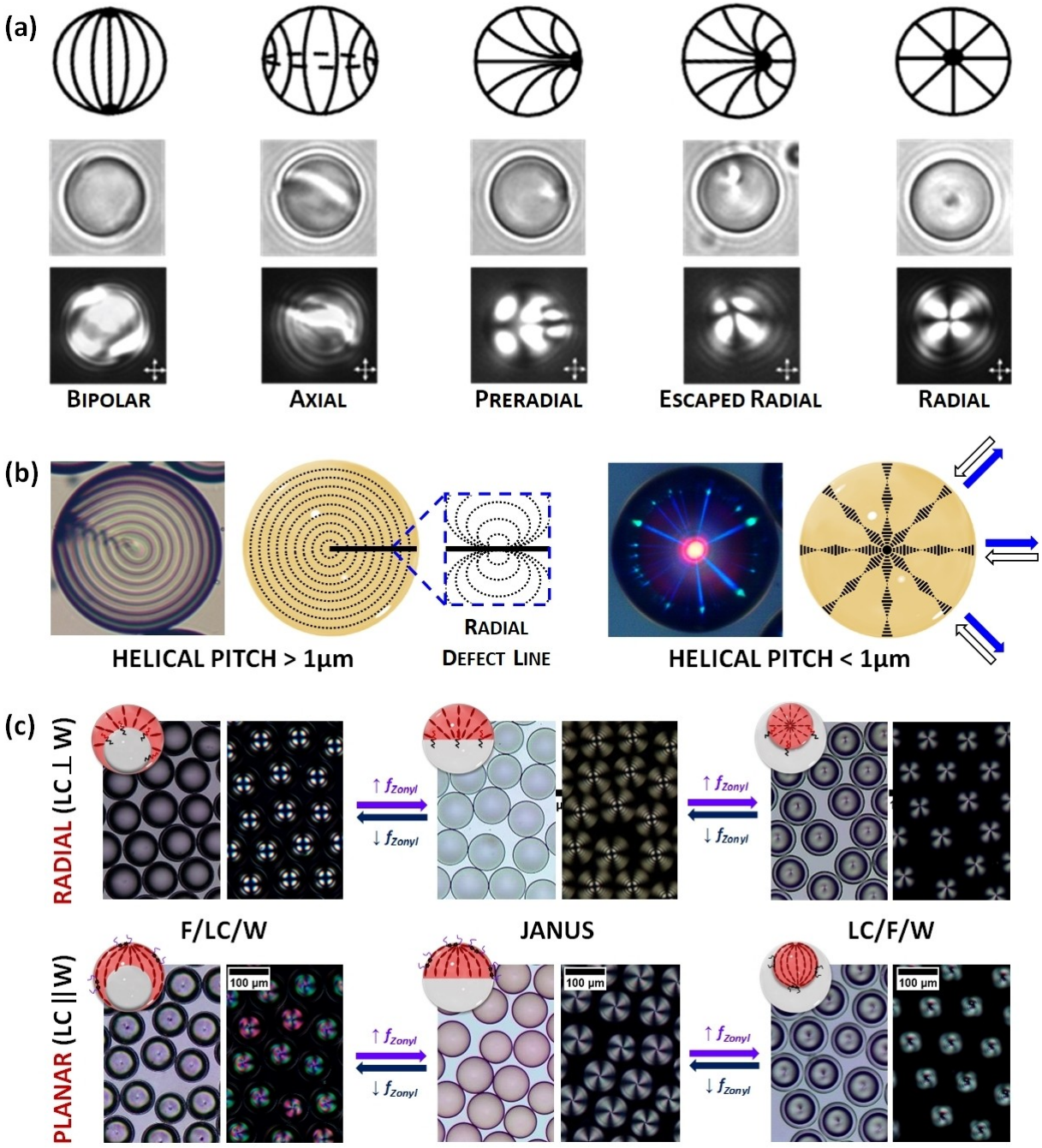

Figure 3. **(a)** Schematic representation (top), bright field (middle), and polarized light (down) images of different LC configurations observed in nematic LC droplets. **(b)** Cholesteric LC droplets with a radial helical organization, in which the mesogens are parallel (planar) to the interface. When the pitch is >1 µm (left), droplets display alternating dark and bright concentric rings and a radial defect line, suggesting a radial disposition of the cholesteric layers following a group of circles that pass through the same point (Frank-Pryce model). When the pitch is in the wavelength range of visible light, droplets show omnidirectional reflection. **(c)** Complex LC emulsions with radial (top) and planar (down) alignment, which dynamically reconfigure in response to surfactant variations between F/LC/W double emulsions, Janus droplets, and LC/F/W double emulsions. Adapted from Refs. [5b, 18b] with permission. Copyright 2014 and 2019 American Chemical Society.

3. Properties of Liquid Crystal Emulsions and Their Applications

LC emulsion droplets offer the versatility to be prepared with various sizes and internal configurations. Additionally, they can incorporate a diverse range of payloads and surfactants, adding extra functionality to the emulsion system. This flexibility enables the creation of LC droplets for a wide array of applications, including: (1) LC emulsions designed to respond to biomolecules, bacteria, or environmental pollutants, making them promising for sensing applications; (2) LC emulsions containing reactive mesogens

that, upon polymerization, yield LC particles with remarkable potential as programmable and reconfigurable microactuators; (3) LC emulsions incorporating cholesteric LC phases that exhibit excellent photonic properties, such as circularly polarized reflection and omnidirectional lasing.

3.1. Chemical and Biological Sensors

LCs have great potential for chemical and biological sensing as the LC orientational order is extremely sensitive to molecular-level interactions occurring at interfaces.[21] The energy required to alter the director field of LC phases is very low, and thus, LC molecules act as amplifiers for local perturbations, which are transmitted from the boundary (i.e., LC interface) into the LC matrix, converting a molecular-level event to an optical texture change that is visible in real time.[22] Changes in LC orientational order generally arise from coupling between the aliphatic tails of the adsorbed foreign molecules and mesogens; this phenomenon is commonly referred as adsorbate-induced ordering transitions. Although LC-based sensors have been traditionally processed in thin film, LC droplets are advantageous for sensing due to their larger specific surface area, their richer configuration textures, and the possibility to generate thermodynamically stable defects.[23] These features, combined with the fact that surfactants are necessary to stabilize LC emulsions, can be used to generate novel LC droplets-based sensors that are triggered in response to interfacial recognition processes for the detection of biomolecules, biomarkers, or organisms.

Abbott and co-workers pioneered the use ordering transitions in micrometer-size LC droplets to detect picogram per milliliter concentrations of endotoxin.[14] The sensitivity of LC droplets showed a six orders of magnitude increase in comparison to that of previously observed with LC thin films, attesting the impact of higher surface area. Similar adsorbate-induced ordering transitions were employed by Abbott, Caruso and co-workers to detect and distinguish between different types of viruses (enveloped and non-enveloped) and bacteria (Gram +ve and −ve).[24] Encapsulated viruses and Gram −ve bacteria present a lipidic envelop that produced bipolar-to-radial transitions when brought into physical contact with LC droplets (Figure 4a).

Another different approach consists of incorporating side-chain LC polymer surfactants functionalized with recognition elements to facilitate ligand-receptor interactions. In this context, several LC emulsion-based sensors were developed to detect cholic acid, enzymatic reactions, DNA, proteins, antibodies, or bacteria.[25] For instance, Kang and co-workers developed LC emulsions for the detection of mouth epidermal carcinoma (KB) or hepatic (HepG2) cancer cells by using amphiphilic block copolymers decorated with folic acid or β-galactose derivatives, respectively.[26] The prepared LC droplets exhibited a radial-to-bipolar transition upon interaction with cancer cells due to interfacial ligand-receptor interactions (Figure 4b). Similarly, LC droplets decorated with poly(*L*-lysine) were employed to detect DNA.[27] Poly(*L*-lysine) induces a radial configuration within droplets, whereas adsorption of double-stranded DNA results in a bipolar configuration. Changes in the LC configuration within droplets can also be triggered by incorporating side-chain LC polymer amphiphiles bearing ionizable groups in the water-soluble block. Specifically, amphiphilic block copolymers with LC and polyacrylic acid blocks (LCP-*b*-PAA) tend to assemble at the LC/W interface and respond reversibly to pH. pH variations trigger changes in the polymeric conformation that strongly influences the anchoring of mesogens at the LC/W interface, producing ordering transitions in LC droplets (Figure 4c). This approach was used to detect glucose, cholesterol, urea, among other biomolecules.[28]

To integrate recognition specificity into LC droplets, several authors identified topological defects as powerful sites for bioconjugation that can cause dramatic changes in the LC director in response to interfacial recognition events.[2b,29] Topological defects have demonstrated ability to host small molecules, particles or amphiphiles and have guided the design of ultrasensitive LC sensors.[21b] In this context, Swager and co-workers developed a new strategy that enabled controlled creation of topological singularities with chemical functionality for the precise attachment of antibodies, thereby providing access multitude of enticing sensing applications.[18b]

Alternatively, cholesteric LC emulsions have also demonstrated utility for the preparation of inexpensive optical sensors that do not require a power source. The selective reflection of cholesteric LCs is directly related to the pitch of its helical organization that can be modified in response to an external stimulus (the analyte in the present case), producing a change in the reflection wavelength (color). This sensing approach was used to detect a variety of analytes ranging from metabolites (e.g., glucose, cholesterol) to carbon dioxide.[30] In both cases, changes in the reflection wavelength were achieved by an analyte-induced physical swelling of the cholesteric helix resulting in a red-shift of the reflection. More recently, Swager and co-workers developed a quantitative detection method based on complex emulsions containing cholesteric LCs.[19] The detection strategy relied on reversible interactions of boronic acid polymeric surfactants with anti-*Salmonella* IgG antibodies at the LC/W interface (Figure 5). Biomolecular recognition events with the foodborne pathogen *Salmonella* could vary the pitch of the cholesteric organization, producing changes in its reflection wavelength.

3.2. Mechanical Actuators

LC elastomers (LCEs) are weakly crosslinked polymers that combine the anisotropic properties of LCs with the rubber elasticity of elastomers.[31] These systems have attracted considerable attention due to their ability to exhibit substantial reversible mechanical deformation in response to external stimuli (Figure 6a). Temperature is the most widely used stimulus, leading to reversible shape changes with the peak deformation occurring at the nematic-to-isotropic

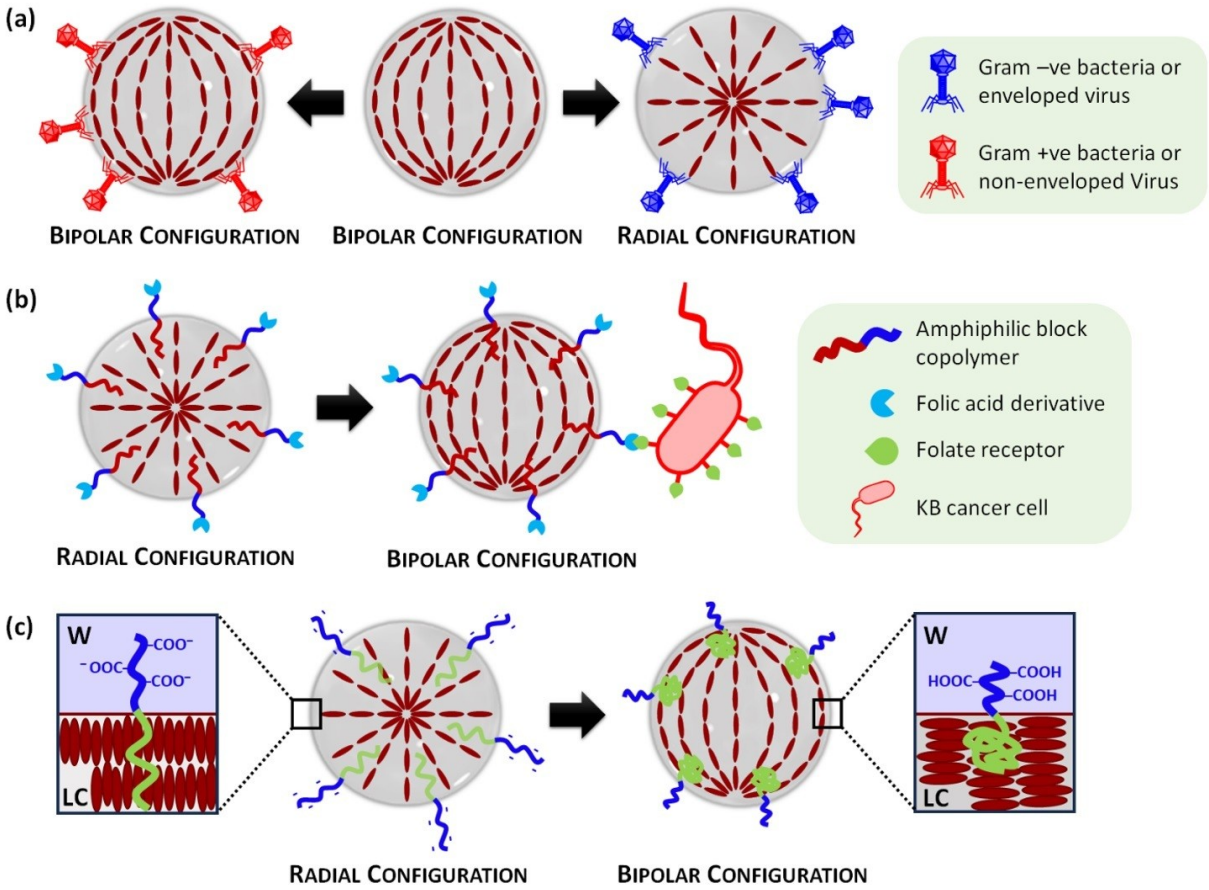

Figure 4. Schematic representation of mechanisms for LC emulsion-based sensors: **(a)** Enveloped viruses or Gram −ve bacteria induce ordering transitions from bipolar to radial upon interaction with LC emulsions. **(b)** Radial-to-bipolar ordering transition induced by the interaction of an amphiphilic block copolymer bearing a terminal folic acid derivative and folate receptors present in KB cancer cells. **(c)** Changes in the conformation of an amphiphilic block copolymer with LC and polyacrylic acid blocks (LCP-*b*-PAA). At high pH values, deprotonation of the carboxylic acids occurs, causing the polymer backbone to spread over a larger area at the LC/W interface, resulting in a homeotropic alignment at interfaces (i.e. radial configuration within droplets). At low pH values, polymer spreads over a small area, inducing a planar alignment of mesogens at the LC/W interface (i.e. bipolar configuration within droplets).

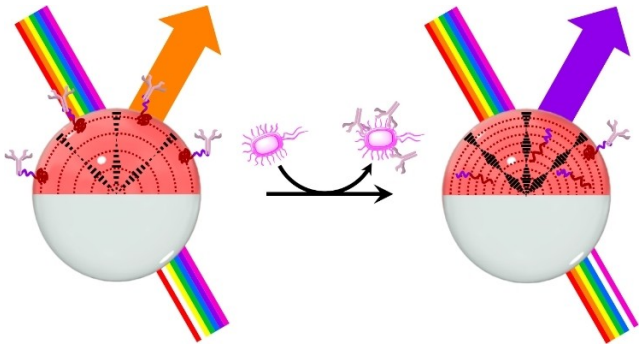

Figure 5. Schematic representation of the mechanism for *Salmonella* detection using cholesteric complex emulsions: changes in reflection are induced by changes in the interfacial activity of boronic acid polymeric surfactants that competitively bind/unbind to IgG antibodies at the LC/W interface. Adapted from Ref. [19] with permission. Copyright 2021 American Chemical Society.

transition.[32] Although the actuation of LCEs was primarily explored in macroscopic films, micrometre-sized actuators are attractive micro-robotic materials for the preparation of valveless micropumps or artificial muscles. LCE microparticles are typically formed through the polymerization of preformed LC emulsion droplets containing polymerizable LC monomers.[33] After the polymerization process, LCE micro-particles are obtained while preserving the inherent LC organization of the precursor LC droplets. This approach facilitates the production of diverse morphologies with precise sizes and controlled LC arrangements within particles, as the initial LC droplets are prepared using the methods previously outlined in Section 2.

The first examples of LCE microspheres were described by Zentel and co-workers and consisted of micrometer-sized particles that showed strong reversible elongation when heated into the isotropic state (Figure 6b).[34] These LCE-based microactuators were prepared by using a T-type microfluidic device, in which droplets based on a polymerizable LCE mixture were in situ photo-crosslinked just after

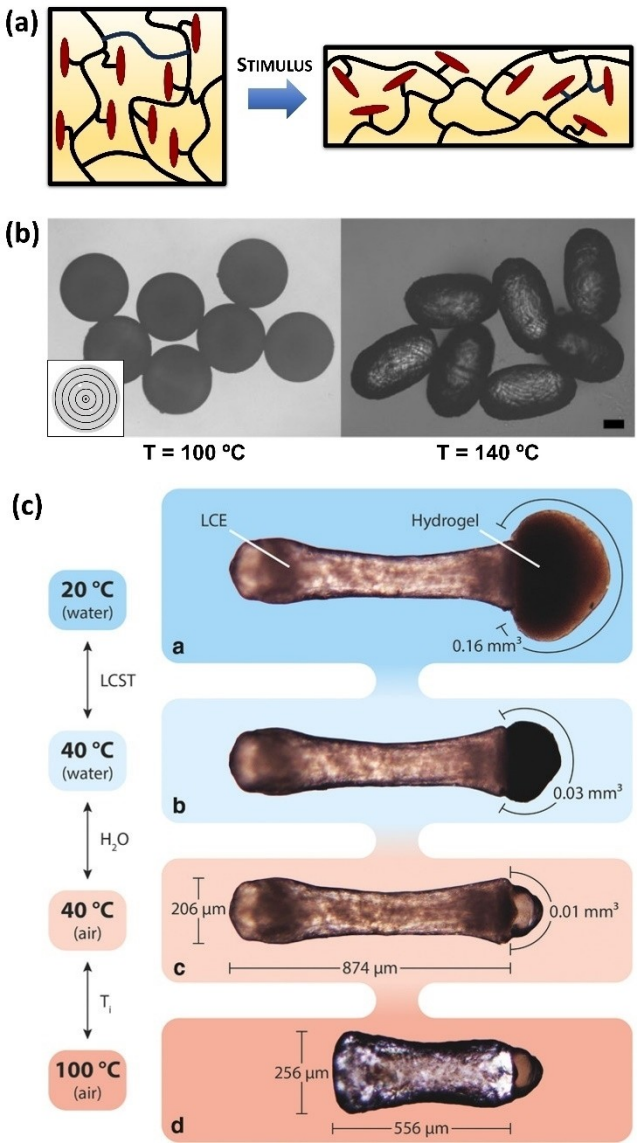

Figure 6. **(a)** Mechanism of LCE actuation: in the LC phase, mesogens force the polymer backbone to adopt a stretched conformation, whereas the polymer assumes a random coiled conformation in the isotropic state. **(b)** LCE particles displaying strong deformation in response to temperature changes (the inset shows the director field orientation within a LCE particle). **(c)** Dual-responsive Janus particles consisting of LCE and hydrogel compartments, with two actuating compartments exhibiting strong shape changes at two different temperatures. Adapted from Refs. [34, 40] with permission. Copyright 2009 and 2018 Wiley-VCH Verlag GmbH & Co. KGaA.

dispersion in an immiscible silicone oil. The size, shape, actuation properties and mechanical robustness of the prepared LCE particles could be readily controlled by a careful selection of the flow rates in the microfluidic device.[35] Moreover, changes in shape could also be produced by swelling LCE particles in a good solvent (e.g., chloroform), which leads to a destruction of the LC order. Such strong actuation properties are the result of a uniform director field configuration, in which LC molecules adopt a concentric alignment within LCE particles (Figure 6b, inset). By incorporating photoresponsive units (e.g., azobenzene derivatives) in the LCE monomer mixture, the nematic to isotropic phase transition could also be photoinduced, thereby producing LCE particles that showed strong and reversible deformation by irradiation with light.[36]

LCEs with more complex morphologies were also developed. For example, Lagerwall, Zentel and co-workers reported core-shell LCE particles prepared by a microfluidic double-emulsion process.[37] The prepared LCE shells containing a liquid core showed temperature-induced actuation during the nematic-to-isotropic transition. This liquid core was reversibly pumped in and out of the particle by actuation of the LCE shell, thereby resulting in a jellyfish-like motion. More recently, Lagerwall and Schenning described LCE shells that exhibited remarkable buckling actuation.[38] The LCE particles were prepared by microfluidics from photocrosslinkable main-chain LC oligomers dissolved in a solvent that was evaporated after the cross-linking process. Actuating Janus particles were also produced by using a dual capillary microfluidic setup combined with photoinitiated radical polymerization.[39] One compartment of the Janus particle comprises a LCE, whereas the other compartment consists of a non-actuating polyacrylamide-based hydrogel. In a subsequent study, they incorporated poly(*N*-isopropylacrylamide) (PNIPAM) hydrogel in the non-LCE compartment, thereby obtaining dual-responsive Janus particles with two actuating compartments (Figure 6c).[40] Specifically, the LCE compartment performed strong temperature-induced shape changes, whereas the PNIPAM part exhibited volumetric expansion due to water swelling at temperatures below the lower critical solution temperature. Interestingly, the authors developed a multi-step molding process to obtain actuating surfaces consisting of a well-packed monolayer of LCE particles.

The previous examples were mainly based on nematic LC organizations. Nonetheless, Schenning and co-workers developed micrometer-sized actuators using cholesteric LC phases. In their first work, they prepared polymerized cholesteric microparticles that showed reversible asymmetric shape deformations combined with structural color changes.[41] They also developed cholesteric polymerized emulsions which showed light-responsive uni- and bidirectional motion and speed control.[42] These micro-sized particles are promising as rotary micromotors and optomechanical transducers.

3.3. Photonic Systems: From Spherical Bragg Reflectors to Omnidirectional Lasers

Cholesteric LCs are extraordinary 1D photonic materials that display light reflection due to their periodic helical organization.[43] Confinement of cholesteric LC phases within micrometer-sized droplets provides unusual functionalities and new potential applications as Bragg reflectors, lasers, or sensors.[44] All these photonic properties require a radial helical orientation of the cholesteric phase within droplets, in which LC molecules are aligned parallel to the aqueous interface. Cholesteric spherical droplets with this

LC arrangement show a characteristic omnidirectional reflection of a constant wavelength, thereby presenting negligible viewing-angle dependance (Figure 7a).[45]

Lagerwall and co-workers demonstrated the unique reflection properties of cholesteric emulsions by preparing a hexagonally close-packed monolayer of monodisperse droplets, which produced colored patterns that result from the omnidirectional reflection of the droplets.[46] These photonic patterns consisted of a central spot from the normal reflection of the cholesteric phase, and several radial reflection lines that correspond to the photonic cross-communication between neighboring droplets (Figure 7b).

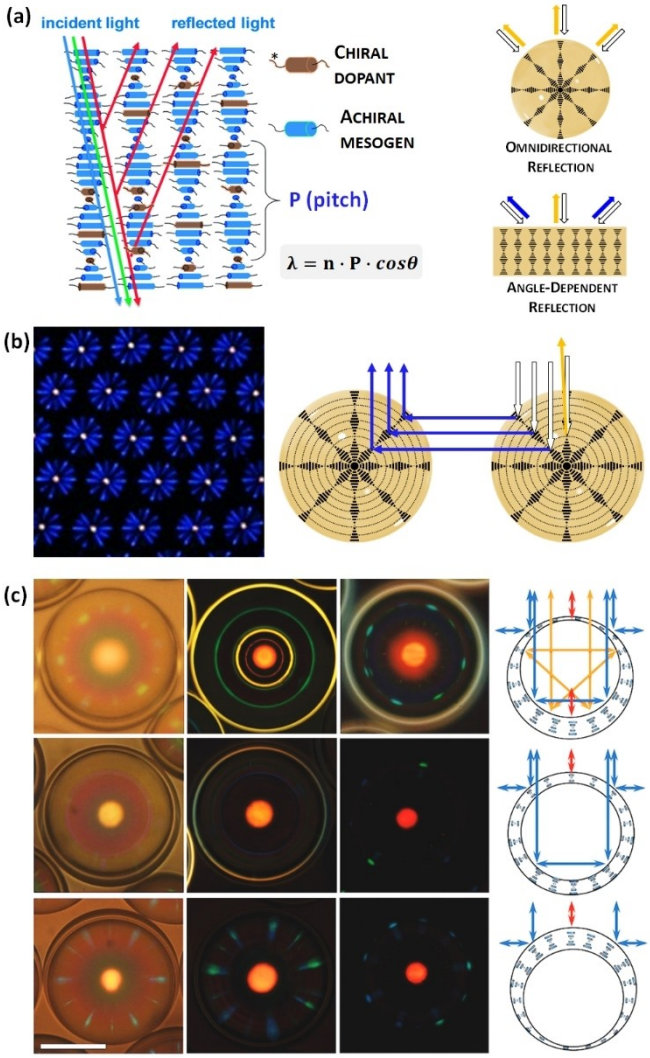

Figure 7. **(a)** Light reflection by a cholesteric LC phase, in which the reflected wavelength (λ) depends on the incidence angle (θ). Cholesteric LC emulsions show angle-independent color of the central reflection. **(b)** Reflection-mode polarized-light optical microscopic image of a monolayer of cholesteric droplets (left), and schematic representation of the photonic cross-communication mechanism between droplets. **(c)** Photonic patterns of planar-aligned cholesteric shells with different compositions and morphologies. Adapted from Ref. [43b] with permission. Copyright 2014 The Royal Society of Chemistry. Adapted from Refs. [47, 55a] with permission. Copyright 2015 and 2018 Wiley-VCH Verlag GmbH & Co. KGaA.

The color of the patterns can be easily controlled by tuning the pitch of the cholesteric LC phase, which is directly related with its selective reflection. To controllably produce intricate multicolor patterns, Li and co-workers prepared cholesteric LC emulsions incorporating a photosensitive chiral molecular switch, which enable obtaining red, green and blue colors from the same droplets by light irradiation.[47] Similarly, Katsonis and co-workers found that the cross-communication phenomenon could be tuned both gradually in wavelength and reversibly in polarization.[48]

To create cholesteric emulsions with additional robustness, solidified (polymerized) particles were fabricated by using reactive LC molecules that were crosslinked to fix the LC arrangement within droplets.[49] This approach offers an increase in stability, extending the utility of cholesteric LC emulsions in applications that may cause breakdown of a pure liquid emulsion. In this context, Schenning and co-workers developed a new approach to produce cholesteric particles that could be easily dispersed in a photo-curable resin to fabricate reflective coatings.[50] Interestingly, they also developed a method to remove cross-communication between particles, obtaining pure structural colors. In a second work, they developed photo- and thermo-responsive photonic coatings based on polymerized cholesteric emulsions that could be brush-painted to prepare stimuli-responsive artistic paintings.[51] Another interesting approach to stabilize cholesteric emulsions consist of dispersing the droplets within a polymer matrix that provide the required mechanical stability.[52] Ye and selected PVA to confine LC droplets and prepare 3D-printed structures with tunable structural color.[53] These systems showed multiple enticing properties, such as tunable color, reversible color change, easy fabrication, and flexible 3D patterning. Alternatively, Kim and co-workers encapsulated each cholesteric droplet within a hydrogel-based membrane to create photonic 'ink' microcapsules that showed remarkable reflection properties and could potentially be used for the construction of a variety of photonic devices.[54]

The aforementioned photonic patterns were also observed in cholesteric shells and were deeply investigated by Lagerwall, Park and co-workers.[55] They performed pioneering research on the different reflection mechanisms involved in shells with different thicknesses, sizes and compositions (Figure 7c). Moreover, they outlined and demonstrated the huge application potential of these dynamic photonic patterns, including retroreflectors, autonomous sensors, high-security identification tags, among others.[56] Li and co-workers fabricated bowl-like shriveled microshells comprising cholesteric LCs. These systems showed a variety of annular structural colors with variable reflection wavelengths and shapes.[57]

Cholesteric emulsions were also widely used for the preparation of omnidirectional microlasers since cholesteric LCs are well-known as mirrorless cavities for lasing.[58] One of the first examples was described by Cipparrone and co-workers.[59] They prepared polymerized cholesteric particles doped with a lasing dye. Omnidirectional lasing occurred, wherein the lasing wavelength depended on the helical pitch of the cholesteric phase. Similarly, Uchida and co-workers

fabricated cholesteric shells that worked as three types of laser resonators for the lasing dye, and the wavelength of operation could be controlled by the LC organization.[60] By incorporating photoresponsive chiral molecular switches into cholesteric shells, Li and co-workers prepared microlasers whose output wavelength could be tuned with light.[61] More recently, Reichmanis and co-workers developed cholesteric shells that serve as resonance cavities for triplet-triplet-annihilation-based photon upconversion (TTA-UC) emission and enables spectral tuning.[62] Moreover, triple-emulsion droplets containing cholesteric LCs with opposite handedness in their core and shell were also developed by Kim and co-workers.[63] These triple emulsions exhibited multiple structural colors due to their dual photonic properties and were used to prepare lasers with two different operating wavelengths.[64]

4. Summary and Outlook

LCs are self-organized materials that have a prominent place in nanoscience, and have found multiple applications in LCD technology, optics, electron/ion transporting materials, etc. Their confinement in spherical geometries (i.e., droplets) has additionally revealed new properties and functions, and has enabled a wealth of unprecedented applications. LC emulsions were designed with diversity of internal LC phases, payloads, and interfacial functionality, that further enrich their unique features. This Minireview summarizes the recent progress in LC emulsions, giving an overall view about their preparation and manipulation, and depicting LC emulsions as valuable candidates for photonics, chemical and biological sensing, and soft robotics. These three applications were selected to illustrate the versatility and smart nature of LC emulsions, but some other applications were also described, including the preparation of nanoporous particles, whispering gallery resonators, or optomechanical systems.

I end by highlighting some unresolved issues and potential opportunities that may influence future research on LC emulsions: (1) Current microfluidic methods enable the production of LC droplets with precise control over size, shape, and internal structure, yet mass production remains a significant challenge. Developing new emulsification strategies that meet real-world industrial demands is needed. Classical polymerization techniques have emerged as a promising approach that can help to address this challenge.[11] (2) Current emulsion systems lack highly complex and active compositions. LC emulsions with increasingly intricate internal organizations and containing stimuli-responsive units holds the potential for the creation of autonomous colloidal systems.[65] (3) LC topological defects serves as three-dimensional templates for the programmable assembly of molecules and (nano)particles.[29,66] Future research should be focused on understanding the potential of topological defect-driven assembly as versatile bottom-up approach for the fabrication of nanoscopic channels to direct transport processes. (4) Although aqueous solutions have been the most widely used continuous phases, some photonic systems exhibit limited performance due to coalescence upon contact with air. Enhancing the stability of photonic devices can be achieved by either polymerizing the LC droplets or utilizing non-polar continuous phases such as silicon oils.[56b,67] (5) LC emulsion-based sensors typically require optical microscopies with crossed polarizers, preventing analyte quantification and restricting their real-world applicability. To simplify the read-out process, future investigations should focus on, for example, developing multichromophore systems that produce emissive signals.

Acknowledgements

This work was supported by the European Union's Horizon 2020 research and innovation program (GA No. 101062667), the "Ramón y Cajal" program (RYC2021-031154-I) funded by MCIN/AEI/10.13039/501100011033 and EU-"NextGenerationEU"/PRTR, and the Gobierno de Aragón-FSE (Research Group E47_23R).

Conflict of Interest

The authors declare no conflict of interest.

Data Availability Statement

Data sharing is not applicable to this article as no new data were created or analyzed in this study.

Keywords: Colloids · Functional Materials · Liquid Crystals · Soft Materials · Supramolecular Chemistry

[1] P. J. Collings, J. W. G. Goodby, *Introduction to liquid crystals : chemistry and physics*, 2nd ed, CRC Press, Boca Raton, Florida, **2019**.
[2] a) H. K. Bisoyi, Q. Li, *Chem. Rev.* **2022**, *122*, 4887–4926; b) Y.-K. Kim, J. Noh, K. Nayani, N. L. Abbott, *Soft Matter* **2019**, *15*, 6913–6929.
[3] a) J. Uchida, B. Soberats, M. Gupta, T. Kato, *Adv. Mater.* **2022**, *34*, 2109063; b) T. Kato, J. Uchida, T. Ichikawa, T. Sakamoto, *Angew. Chem. Int. Ed.* **2018**, *57*, 4355–4371.
[4] a) M. Urbanski, C. G. Reyes, J. Noh, A. Sharma, Y. Geng, V. Subba Rao Jampani, J. P. F. Lagerwall, *J. Condens. Matter Phys.* **2017**, *29*, 133003; b) T. Lopez-Leon, A. Fernandez-Nieves, *Colloid Polym. Sci.* **2011**, *289*, 345–359.
[5] a) H.-Q. Chen, X.-Y. Wang, H. K. Bisoyi, L.-J. Chen, Q. Li, *Langmuir* **2021**, *37*, 3789–3807; b) D. S. Miller, X. Wang, N. L. Abbott, *Chem. Mater.* **2014**, *26*, 496–506.
[6] R. V. Balaj, L. D. Zarzar, *Chem. Phys. Rev.* **2020**, *1*, 011301.
[7] X. Wang, E. Bukusoglu, N. L. Abbott, *Chem. Mater.* **2017**, *29*, 53–61.
[8] T. F. Tadros, *Emulsions: Formation, Stability, Industrial Applications*, de Gruyter GmbH, Berlin, **2016**.
[9] a) J. K. Gupta, S. Sivakumar, F. Caruso, N. L. Abbott, *Angew. Chem. Int. Ed.* **2009**, *48*, 1652–1655; b) F. Caruso, R. A. Caruso, H. Möhwald, *Science* **1998**, *282*, 1111–1114.
[10] a) S. Battat, D. A. Weitz, G. M. Whitesides, *Lab Chip* **2022**, *22*, 530–536; b) L. Shang, Y. Cheng, Y. Zhao, *Chem. Rev.* **2017**,

117, 7964–8040; c) C.-H. Choi, J. Kim, J.-O. Nam, S.-M. Kang, S.-G. Jeong, C.-S. Lee, *ChemPhysChem* **2014**, *15*, 21–29.
[11] X. Liu, M. G. Debije, J. P. A. Heuts, A. P. H. J. Schenning, *Chem. Eur. J.* **2021**, *27*, 14168–14178.
[12] X. Liu, Y. Xu, J. P. A. Heuts, M. G. Debije, A. P. H. J. Schenning, *Macromolecules* **2019**, *52*, 8339–8345.
[13] D. S. Miller, R. J. Carlton, P. C. Mushenheim, N. L. Abbott, *Langmuir* **2013**, *29*, 3154–3169.
[14] I.-H. Lin, D. S. Miller, P. J. Bertics, C. J. Murphy, J. J. de Pablo, N. L. Abbott, *Science* **2011**, *332*, 1297–1300.
[15] a) V. Tomar, S. I. Hernández, N. L. Abbott, J. P. Hernández-Ortiz, J. J. de Pablo, *Soft Matter* **2012**, *8*, 8679–8689; b) J. K. Gupta, J. S. Zimmerman, J. J. de Pablo, F. Caruso, N. L. Abbott, *Langmuir* **2009**, *25*, 9016–9024; c) E. Tjipto, K. D. Cadwell, J. F. Quinn, A. P. R. Johnston, N. L. Abbott, F. Caruso, *Nano Lett.* **2006**, *6*, 2243–2248.
[16] a) J. Noh, B. Henx, J. P. F. Lagerwall, *Adv. Mater.* **2016**, *28*, 10170–10174; b) H.-L. Liang, S. Schymura, P. Rudquist, J. Lagerwall, *Phys. Rev. Lett.* **2011**, *106*, 247801.
[17] D. A. Paterson, X. Du, P. Bao, A. A. Parry, S. A. Peyman, J. A. T. Sandoe, S. D. Evans, D. Luo, R. J. Bushby, J. C. Jones, H. F. Gleeson, *Mol. Syst. Des. Eng.* **2022**, *7*, 607–621.
[18] a) C. A. Zentner, A. Concellón, T. M. Swager, *ACS Cent. Sci.* **2020**, *6*, 1460–1466; b) A. Concellón, C. A. Zentner, T. M. Swager, *J. Am. Chem. Soc.* **2019**, *141*, 18246–18255.
[19] A. Concellón, D. Fong, T. M. Swager, *J. Am. Chem. Soc.* **2021**, *143*, 9177–9182.
[20] X. Liu, M.-A. Moradi, T. Bus, M. G. Debije, S. A. F. Bon, J. P. A. Heuts, A. P. H. J. Schenning, *Angew. Chem. Int. Ed.* **2021**, *60*, 27026–27030.
[21] a) Z. Wang, T. Xu, A. Noel, Y.-C. Chen, T. Liu, *Soft Matter* **2021**, *17*, 4675–4702; b) K. Nayani, Y. Yang, H. Yu, P. Jani, M. Mavrikakis, N. Abbott, *Liq. Cryst. Today* **2020**, *29*, 24–35; c) R. J. Carlton, J. T. Hunter, D. S. Miller, R. Abbasi, P. C. Mushenheim, L. N. Tan, N. L. Abbott, *Liq. Cryst. Rev.* **2013**, *1*, 29–51; d) A. M. Lowe, N. L. Abbott, *Chem. Mater.* **2012**, *24*, 746–758.
[22] a) E. Bukusoglu, M. B. Pantoja, P. C. Mushenheim, X. Wang, N. L. Abbott, *Annu. Rev. Chem. Biomol. Eng.* **2016**, *7*, 163–196; b) D. Wang, S.-Y. Park, I.-K. Kang, *J. Mater. Chem. C* **2015**, *3*, 9038–9047.
[23] R. Xie, N. Li, Z. Li, J. Chen, K. Li, Q. He, L. Liu, S. Zhang, *Biosensors* **2022**, *12*, 758.
[24] S. Sivakumar, K. L. Wark, J. K. Gupta, N. L. Abbott, F. Caruso, *Adv. Funct. Mater.* **2009**, *19*, 2260–2265.
[25] a) I. Pani, F. N. K. M., M. Sharma, S. K. Pal, *Nano Lett.* **2021**, *21*, 4546–4553; b) B. J. Ortiz, M. E. Boursier, K. L. Barrett, D. E. Manson, D. Amador-Noguez, N. L. Abbott, H. E. Blackwell, D. M. Lynn, *ACS Appl. Mater. Interfaces* **2020**, *12*, 29056–29065; c) P. Bao, D. A. Paterson, P. L. Harrison, K. Miller, S. Peyman, J. C. Jones, J. Sandoe, S. D. Evans, R. J. Bushby, H. F. Gleeson, *Lab Chip* **2019**, *19*, 1082–1089; d) K. Lee, K. C. Gupta, S.-Y. Park, I.-K. Kang, *J. Mater. Chem. B* **2016**, *4*, 704–715; e) J. Deng, X. Lu, C. Constant, A. Dogariu, J. Fang, *Chem. Commun.* **2015**, *51*, 8912–8915; f) M. Khan, S.-Y. Park, *Colloids Surf. B* **2015**, *127*, 241–246.
[26] a) Y. Choi, K. Lee, K. C. Gupta, S.-Y. Park, I.-K. Kang, *J. Mater. Chem. B* **2015**, *3*, 8659–8669; b) S. H. Yoon, K. C. Gupta, J. S. Borah, S.-Y. Park, Y.-K. Kim, J.-H. Lee, I.-K. Kang, *Langmuir* **2014**, *30*, 10668–10677.
[27] I. Verma, S. Sidiq, S. K. Pal, *ACS Omega* **2017**, *2*, 7936–7945.
[28] a) M. Khan, S.-Y. Park, *Sens. Actuators B* **2014**, *202*, 516–522; b) J. Kim, M. Khan, S.-Y. Park, *ACS Appl. Mater. Interfaces* **2013**, *5*, 13135–13139; c) W. Khan, S.-Y. Park, *Lab Chip* **2012**, *12*, 4553–4559; d) W. Khan, J. H. Choi, G. M. Kim, S.-Y. Park, *Lab Chip* **2011**, *11*, 3493–3498.
[29] X. Wang, D. S. Miller, E. Bukusoglu, J. J. de Pablo, N. L. Abbott, *Nat. Mater.* **2016**, *15*, 106.
[30] a) L. Pschyklenk, T. Wagner, A. Lorenz, P. Kaul, *ACS Appl. Polym. Mater.* **2020**, *2*, 1925–1932; b) H.-G. Lee, S. Munir, S.-Y. Park, *ACS Appl. Mater. Interfaces* **2016**, *8*, 26407–26417.
[31] a) M. Pilz da Cunha, M. G. Debije, A. P. H. J. Schenning, *Chem. Soc. Rev.* **2020**, *49*, 6568–6578; b) Y. Shang, J. Wang, T. Ikeda, L. Jiang, *J. Mater. Chem. C* **2019**, *7*, 3413–3428.
[32] K. Mehta, A. R. Peeketi, L. Liu, D. Broer, P. Onck, R. K. Annabattula, *Appl. Phys. Rev.* **2020**, *7*, 041306.
[33] L. B. Braun, R. Zentel, *Liq. Cryst.* **2019**, *46*, 2023–2041.
[34] C. Ohm, C. Serra, R. Zentel, *Adv. Mater.* **2009**, *21*, 4859–4862.
[35] C. Ohm, E.-K. Fleischmann, I. Kraus, C. Serra, R. Zentel, *Adv. Funct. Mater.* **2010**, *20*, 4314–4322.
[36] a) D. Ditter, P. Blümler, B. Klöckner, J. Hilgert, R. Zentel, *Adv. Funct. Mater.* **2019**, *29*, 1902454; b) L. B. Braun, T. Hessberger, R. Zentel, *J. Mater. Chem. C* **2016**, *4*, 8670–8678.
[37] E.-K. Fleischmann, H.-L. Liang, N. Kapernaum, F. Giesselmann, J. Lagerwall, R. Zentel, *Nat. Commun.* **2012**, *3*, 1178.
[38] V. S. R. Jampani, D. J. Mulder, K. R. De Sousa, A.-H. Gélébart, J. P. F. Lagerwall, A. P. H. J. Schenning, *Adv. Funct. Mater.* **2018**, *28*, 1801209.
[39] T. Hessberger, L. B. Braun, F. Henrich, C. Müller, F. Gießelmann, C. Serra, R. Zentel, *J. Mater. Chem. C* **2016**, *4*, 8778–8786.
[40] T. Hessberger, L. B. Braun, R. Zentel, *Adv. Funct. Mater.* **2018**, *28*, 1800629.
[41] A. Belmonte, Y. Y. Ussembayev, T. Bus, I. Nys, K. Neyts, A. P. H. J. Schenning, *Small* **2020**, *16*, 1905219.
[42] Y. Y. Ussembayev, N. De Witte, X. Liu, A. Belmonte, T. Bus, S. Lubach, F. Beunis, F. Strubbe, A. P. H. J. Schenning, K. Neyts, *Small* **2023**, *19*, 2207095.
[43] a) L. Wang, A. M. Urbas, Q. Li, *Adv. Mater.* **2020**, *32*, 1801335; b) D. J. Mulder, A. P. H. J. Schenning, C. W. M. Bastiaansen, *J. Mater. Chem. C* **2014**, *2*, 6695–6705.
[44] Z.-G. Zheng, Y.-Q. Lu, Q. Li, *Adv. Mater.* **2020**, *32*, 1905318.
[45] E. Beltran-Gracia, O. L. Parri, *J. Mater. Chem. C* **2015**, *3*, 11335–11340.
[46] J. Noh, H.-L. Liang, I. Drevensek-Olenik, J. P. F. Lagerwall, *J. Mater. Chem. C* **2014**, *2*, 806–810.
[47] J. Fan, Y. Li, H. K. Bisoyi, R. S. Zola, D.-k. Yang, T. J. Bunning, D. A. Weitz, Q. Li, *Angew. Chem. Int. Ed.* **2015**, *54*, 2160–2164.
[48] S. J. Aβhoff, S. Sukas, T. Yamaguchi, C. A. Hommersom, S. Le Gac, N. Katsonis, *Sci. Rep.* **2015**, *5*, 14183.
[49] H. J. Seo, S. S. Lee, J. Noh, J.-W. Ka, J. C. Won, C. Park, S.-H. Kim, Y. H. Kim, *J. Mater. Chem. C* **2017**, *5*, 7567–7573.
[50] A. Belmonte, T. Bus, D. J. Broer, A. P. H. J. Schenning, *ACS Appl. Mater. Interfaces* **2019**, *11*, 14376–14382.
[51] A. Belmonte, M. Pilz da Cunha, K. Nickmans, A. P. H. J. Schenning, *Adv. Opt. Mater.* **2020**, *8*, 2000054.
[52] a) Q. Yan, Z. Wei, P. Lin, Z. Cheng, M. Pu, Z. Huang, W. Lin, *Opt. Mater. Express* **2018**, *8*, 1536–1550; b) G. Petriashvili, M. P. De Santo, R. J. Hernandez, R. Barberi, G. Cipparrone, *Soft Matter* **2017**, *13*, 6227–6233.
[53] C. Yang, B. Wu, J. Ruan, P. Zhao, L. Chen, D. Chen, F. Ye, *Adv. Mater.* **2021**, *33*, 2006361.
[54] S. S. Lee, B. Kim, S. K. Kim, J. C. Won, Y. H. Kim, S.-H. Kim, *Adv. Mater.* **2015**, *27*, 627–633.
[55] a) Y. Geng, J.-H. Jang, K.-G. Noh, J. Noh, J. P. F. Lagerwall, S.-Y. Park, *Adv. Opt. Mater.* **2018**, *6*, 1700923; b) J.-G. Kim, S.-Y. Park, *Adv. Opt. Mater.* **2017**, *5*, 1700243; c) Y. Geng, J. Noh, I. Drevensek-Olenik, R. Rupp, G. Lenzini, J. P. F. Lagerwall, *Sci. Rep.* **2016**, *6*, 26840.
[56] a) H. Agha, Y. Geng, X. Ma, D. I. Avşar, R. Kizhakidathazhath, Y.-S. Zhang, A. Tourani, H. Bavle, J.-L. Sanchez-Lopez, H. Voos, M. Schwartz, J. P. F. Lagerwall, *Light-Sci. Appl.* **2022**,

11, 309; b) M. Schwartz, G. Lenzini, Y. Geng, P. B. Rønne, P. Y. A. Ryan, J. P. F. Lagerwall, *Adv. Mater.* **2018**, *30*, 1707382.
[57] Y.-W. Shan, L.-Q. You, H. K. Bisoyi, Y.-J. Yang, Y.-H. Ge, K.-J. Che, S.-S. Li, L.-J. Chen, Q. Li, *Adv. Opt. Mater.* **2020**, *8*, 2000692.
[58] J. Ortega, C. L. Folcia, J. Etxebarria, *Materials* **2018**, *11*, 5.
[59] G. Cipparrone, A. Mazzulla, A. Pane, R. J. Hernandez, R. Bartolino, *Adv. Mater.* **2011**, *23*, 5773–5778.
[60] Y. Uchida, Y. Takanishi, J. Yamamoto, *Adv. Mater.* **2013**, *25*, 3234–3237.
[61] L. Chen, Y. Li, J. Fan, H. K. Bisoyi, D. A. Weitz, Q. Li, *Adv. Opt. Mater.* **2014**, *2*, 845–848.
[62] J.-H. Kang, S.-H. Kim, A. Fernandez-Nieves, E. Reichmanis, *J. Am. Chem. Soc.* **2017**, *139*, 5708–5711.
[63] S. S. Lee, H. J. Seo, Y. H. Kim, S.-H. Kim, *Adv. Mater.* **2017**, *29*, 1606894.
[64] S. Park, S. S. Lee, S.-H. Kim, *Adv. Mater.* **2020**, *32*, 2002166.
[65] a) R. Zhang, A. Mozaffari, J. J. de Pablo, *Nat. Rev. Mater.* **2021**, *6*, 437–453; b) R. Zheng, L. Ma, W. Feng, J. Pan, Z. Wang, Z. Chen, Y. Zhang, C. Li, P. Chen, H. K. Bisoyi, B. Li, Q. Li, Y. Lu, *Adv. Funct. Mater.* **2023**, 2301142.
[66] F. Mondiot, X. Wang, J. J. de Pablo, N. L. Abbott, *J. Am. Chem. Soc.* **2013**, *135*, 9972–9975.
[67] S. Lin, Y. Tang, W. Kang, H. K. Bisoyi, J. Guo, Q. Li, *Nat. Commun.* **2023**, *14*, 3005.

Manuscript received: June 23, 2023
Accepted manuscript online: September 11, 2023
Version of record online: September 18, 2023